The Linnean Society of London BIOLOGICAL Journal of the Linnean Society

Biological Journal of the Linnean Society, 2016, ••, ••–••. With 7 figures.

Comparative anatomy of the bony labyrinth of extant and extinct porpoises (Cetacea: Phocoenidae)

RACHEL A. RACICOT[1,2]*, WILLIAM GEARTY[3], NAOKI KOHNO[4,5] and JOHN J. FLYNN[6,7]

[1]*The Dinosaur Institute, Natural History Museum of Los Angeles County, Los Angeles, CA, USA*
[2]*Smithsonian Institution, P. O. Box 37012, MRC 121, Washington, DC, 20013–7012, USA*
[3]*Department of Geological Sciences, Stanford University, Stanford, CA, USA*
[4]*Department of Geology and Paleontology, Division of Biotic Evolution, National Museum of Nature and Science, Tokyo, Japan*
[5]*Graduate School of Life and Environmental Sciences, University of Tsukuba, Japan*
[6]*Department of Vertebrate Paleontology, Division of Paleontology, American Museum of Natural History, New York, NY, USA*
[7]*Richard Gilder Graduate School, American Museum of Natural History, New York, NY, USA*

Received 4 February 2016; revised 18 May 2016; accepted for publication 19 May 2016

The inner ear anatomy of cetaceans, now more readily accessible by means of nondestructive high-resolution X-ray computed tomographic (CT) scanning, provides a window into their acoustic abilities and ecological preferences. Inner ear labyrinths also may be a source for additional morphological characters for phylogenetic analyses. In this study, we explore digital endocasts of the inner ear labyrinths of representative species of extinct and extant porpoises (Mammalia: Cetacea: Phocoenidae), a clade of some of the smallest odontocete cetaceans, which produce some of the highest-frequency clicks for biosonar and communication. Metrics used to infer hearing ranges based on cochlear morphology indicate that all taxa considered could hear high-frequency sounds, thus the group had already acquired high-frequency hearing capabilities by the Miocene (9–11 Mya) at the latest. Vestibular morphology indicates that extant species with pelagic preferences have similarly low semicircular canal deviations from 90°, values indicating more sensitivity to head rotations. Species with near-shore preferences have higher canal deviation values, indicating less sensitivity to head rotations. Extending these analyses to the extinct species, we demonstrate a good match between those predicted to have coastal (such as *Semirostrum cerutti*) preferences and high canal deviation values. We establish new body length relationships based on correlations with inner ear labyrinth volume, which can be further explored among other aquatic mammals to infer body size of specimens consisting of fragmentary material. © 2016 The Linnean Society of London, *Biological Journal of the Linnean Society*, 2016, **00**, 000–000.

KEYWORDS: auditory acuity – Cetacea – CT scan – inner ear.

INTRODUCTION

The mammalian inner ear labyrinth has garnered scientific interest since the late 19th century, and more recently computed tomographic (CT) scans have allowed the unprecedented exploration of this region (e.g., Geisler & Luo, 1996; Spoor *et al.*, 2002; Yamato *et al.*, 2008; Macrini *et al.*, 2010, 2013; Ni, Flynn & Wyss, 2010; Ekdale, 2013; Gutstein *et al.*, 2014; Ekdale & Racicot, 2015; Grohé *et al.*, 2015). Odontocete (Cetacea: Odontoceti) hearing in general has received a great deal of attention because of interest in studying anatomical modifications associated with echolocation in mammals (e.g., Ketten & Wartzok, 1990; Luo & Eastman, 1995; Cranford, Krysl & Amundin, 2010; Houser *et al.*, 2010; Park, Fitzgerald & Evans, 2016), but few studies exist that have specifically explored the inner ear labyrinths at fine taxonomic resolution within major clades. Because variation in both the cochlea and vestibule may provide insight into physiological evolution, studies of specific clades of animals, and particularly cetaceans, become increasingly important especially in the context of how these animals evolved during dramatic

*Corresponding author. E-mail: rracicot@nhm.org

global environmental changes and how a better understanding of these evolutionary events informs conservation of rare extant species. Of particular interest is the evolution of narrow-band high-frequency sound production and hearing that is specific to only a few odontocete clades, including phocoenids and their ecologically similar delphinid relatives such as Commerson's dolphin (*Cephalorhynchus commersonii* Lacépède, 1804), the dwarf and pygmy sperm whales (*Kogia* Gray, 1846), and the small river dolphin species *Pontoporia blainvillei* Gervais & d'Orbigny, 1844 (Anderson & Amundin, 1976; Morisaka & Connor, 2007; Miller & Wahlberg, 2013). The evolution of specialized, narrow-band, high-frequency hearing in phocoenids (Morisaka & Connor, 2007) is a topic of interest as to how it relates to their ecology and conservation; morphology of the inner ear labyrinths can provide insight into this aspect of their evolution. This study is the first, to our knowledge, to explore morphological characteristics of the inner ear of extant and extinct phocoenids and the ecologically similar delphinid (outgroup), *C. commersonii*, to address questions surrounding the evolution of high-frequency hearing, along with other aspects of inner ear morphology and function in cetaceans.

Inner ear labyrinth morphology, as an integral aspect of the sensory systems of cetaceans, is linked to important aspects of delphinoid (Cetacea: Delphinoidea) behaviour and survival such as navigating, finding prey, and detecting predators (Mooney, Yamato & Branstetter, 2012), and has the potential to be phylogenetically informative. Although characteristics from osseous external ear morphology are commonly used in mammalian systematics, the investigation of three-dimensional (3D) inner ear morphology has received less attention historically owing to primarily destructive access to this region (although see Ekdale, 2010; Morell *et al.*, 2007; Sensor *et al.*, 2015; Yamato *et al.*, 2008). Morphological aspects of the cochlea have been shown to correlate with hearing and auditory acuity (Parks *et al.*, 2007; Manoussaki *et al.*, 2008), and measurements based on this region have been used to infer hearing capability in extinct whales (e.g., Luo & Eastman, 1995; Geisler & Luo, 1996; Luo & Marsh, 1996; Ekdale & Racicot, 2015). Features of the cochlea related to hearing capability include the basilar membrane length and width and the number of turns of the cochlear spiral, all of which are thought to correlate with the range of high- and low-frequency hearing (Wever *et al.*, 1971; Wever, 1972). For example, an increased number of turns of the cochlea (and thus increased cochlear length) implies lower frequency hearing, whereas fewer cochlear turns and shorter cochlear lengths are associated with high-frequency hearing. The basilar membrane, a soft tissue structural component of the cochlea, the width of which is correlated with hearing frequencies (thinner = higher frequency), is often damaged or destroyed in preparation of recent specimens, and is always destroyed during fossilization. Bony proxies such as laminar gap width and approximations of this measurement when the structure is not axially preserved (e.g., extent of the radial base of the secondary bony lamina and 'whole laminar gap width'), along with a combination of other morphology-based proxies, including several ratios that describe the shape of the cochlear spiral, can be used (Geisler & Luo, 1996; Ekdale & Racicot, 2015). The ratio of the radii at the apex and base of the cochlear spiral recently was shown to predict the low-frequency hearing limits of mammals (Manoussaki *et al.*, 2008), although 'specialist' species such as phocoenids were not included. Elucidating the ancestral hearing capabilities in phocoenids is facilitated by comparing fossils with extant taxa, in a phylogenetic framework, which can better inform our understanding of changes in ecological patterns through time (e.g., adaptations to avoid larger predators by echolocating at frequencies higher than predators can hear; Anderson & Amundin, 1976; Morisaka & Connor, 2007) and the evolution of specialized high-frequency hearing in general. High-resolution X-ray CT scans, and the 'virtual' extraction of inner ear cavities and their morphologies, therefore offer a unique and unprecedented opportunity to study the evolution and function of physiologically important features of the inner ear labyrinths.

The vestibular region, associated with senses of space and balance, has been shown to become smaller as whales transitioned to fully aquatic lifestyles (Spoor *et al.*, 2002), but the vestibular morphological change at interspecific scales within particular clades has not been studied. Further, the potential utility of the vestibule as a source of phylogenetic and physiological inferences has not been explored in detail in cetaceans, partly due to the unavailability of high-resolution CT scans and more academic interest in the cochlea and hearing in whales. Semicircular canal dimensions and overall inner ear labyrinth size may be useful for inferring the ecology and evolution of extinct species based on evidence from the extant groups. The ability to infer ecology and body size using the inner ear labyrinths of phocoenids is particularly useful because periotics tend to preserve well in the fossil record, and may sometimes be the only representation of an extinct species. This study is the first to include a comprehensive sampling of fossil and recent phocoenid specimens (all known extant species and nine extinct species) with well resolved vestibular, as well as cochlear, morphology to address questions about hearing, apomorphy acquisition, and possible ecological preferences in extinct and extant porpoises.

MATERIAL AND METHODS

Specimens

We analyzed 19 individual tympanoperiotics or periotics (ear bones, or petrosals) for this study (see Supporting Information, Table S1 for museum institutional abbreviations and catalogue numbers); these included all ($N = 6$) known extant phocoenid species (including one adult and one juvenile *Phocoena phocoena* Linnaeus, 1758), and nine fossil specimens. In addition to these specimens, we analyzed one delphinid species (*C. commersonii*), which is considered to be convergent in morphology with porpoises (particularly those that prefer coastal habitats such as *P. phocoena*) because of their similar paedomorphic characteristics, small size, and narrow-band, high-frequency sound production (see Galatius, 2010). Recent specimens were selected from museum collections for scanning based on availability, genotype-based phylogenetic affinity, and condition (i.e., paired, complete tympanoperiotic complexes when possible). Locality and life history information were not available for all specimens, especially for the rare extant species and fossil specimens. Both the left and right tympanoperiotics were scanned whenever possible. The fossil specimens (representing *Haborophocoena toyoshimai* Ichishima & Kimura, 2005; *Numataphocoena yamashitai* Ichishima & Kimura, 2000; *Miophocaena nishinoi* Murakami *et al.*, 2012; *Piscolithax boreios* Barnes, 1984; *Piscolithax tedfordi* Barnes, 1984; *Pterophocaena nishinoi* Murakami *et al.*, 2012; *Salumiphocaena stocktoni* Wilson, 1973; *Semirostrum ceruttii* Racicot *et al.*, 2014; and an undescribed Phocoenidae cf., referred as Phocoenidae unnamed genus 1 in Boessenecker, 2013) were selected based on availability, their inclusion in recent morphology-based phylogenetic studies (Murakami *et al.*, 2012a, b, 2015; Racicot *et al.*, 2014), and the potential for discovery of additional phylogenetic characters and functional correspondences with modern species.

Computed tomography methods

Specimens were CT scanned at the University of Texas High-Resolution X-Ray CT facility (UTCT), the American Museum of Natural History Microscopy and Imaging Facility (MIF), and the National Museum of Nature and Science Imaging Facility, Tokyo (see Supporting Information, Table S1 for scanning parameters for each specimen). Digital endocasts of the inner ear labyrinths were extracted using VGStudioMAX 2.2 (Fig. 1). Because the delicate structures delineating the spiral ganglion canals were sometimes broken or incomplete (especially in fossils), segmentation of the cochlea includes the spiral ganglion canal in this study. Anterior and dorsal views of the inner ear labyrinths were oriented with the anterior canal positioned vertically along the dorsoventral axis. Some fossil specimens reflect incomplete anatomical preservation due to breakage or diagenesis. Most notably, *M. nishinoi* is missing portions of the lateral canal of the vestibule and fenestra vestibuli, and portions of the canaliculus cochleae appear to have been broken and recrystallized. The cast of the aqueductus vestibuli was not included in the extraction of all endocasts due to its minute size internally, but is visible in most of the

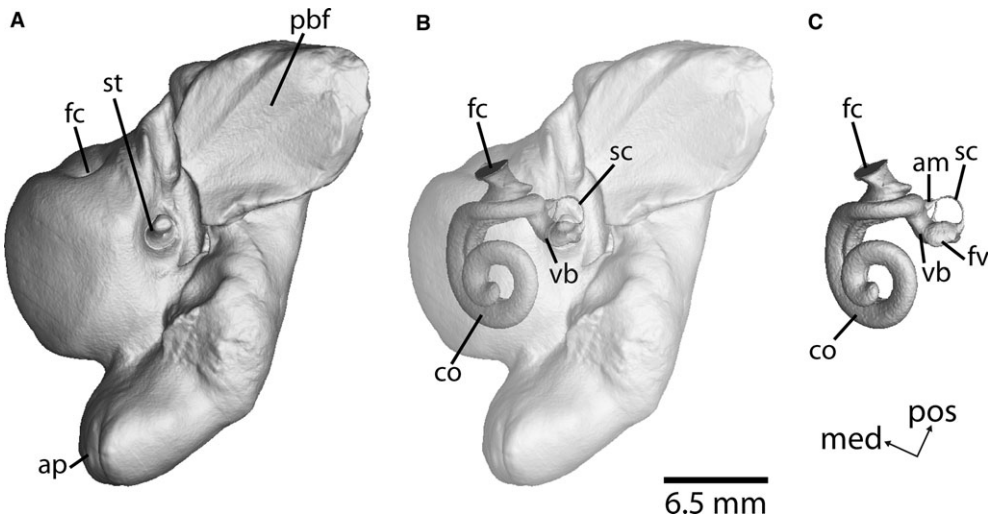

Figure 1. Digital isosurfaces of the right periotic of *Salumiphocaena stocktoni*, oriented in the same position for each part of the figure. A, tympanic view of the periotic/petrosal bone. B, periotic rendered semitransparent with the bony labyrinth endocast rendered at 100% opacity. C, endocast of bony labyrinth. Abbreviations listed at the end of the materials and methods section.

CT scans and referred to in the text when pertinent. The cast of the canaliculus cochleae was cut off at or just before reaching the fenestra cochleae, using the 3D Polyline tool in VGStudioMAX 2.2, thus the lengths of the canaliculus shown in figures reflect approximate actual lengths of the canaliculus cochleae. The original CT data in TIFF stacks as well as STL files of the inner ear labyrinth casts will be provided on MorphoSource or can be requested directly from the corresponding author.

Measurement methods

Several measurements were obtained to assess the variation within the sample of specimens (Supporting Information, Tables S2–S5; Fig. 2), following the methods of previous studies (Berlin, Kirk & Rowe, 2013; Ekdale, 2013; Ekdale & Racicot, 2015; Ekdale & Rowe, 2011; Macrini *et al.*, 2013; Spoor *et al.*, 2007). Cochlear height and width measurements, along with counts of spiral turns, were taken using ImageJ on images with scale bars obtained in VGStudioMAX 2.2. Otherwise, measurements were taken directly on the digital endocast using the 'caliper' or 'Polyline' tools in VGStudioMAX 2.2. Volume and surface area measurements of the cochlea and vestibule, used as general estimates of size for comparison with body mass and length, were obtained using 'object properties' options in VGStudioMAX 2.2. The vestibule was digitally isolated from the cochlea at the medial border of the fenestra vestibuli using the Polyline 3D tool to maintain consistency in volumetric measurements. The whole volume of the inner ear labyrinth of each specimen includes the canaliculus cochleae. The endocasts were extracted from VGStudioMAX 2.2 as TIFF stacks and loaded along with the original CT data into Avizo 6.0 for additional measurements such as the internal dimensions of the cochlea at every quarter turn, graded ratio, and semicircular canal angles.

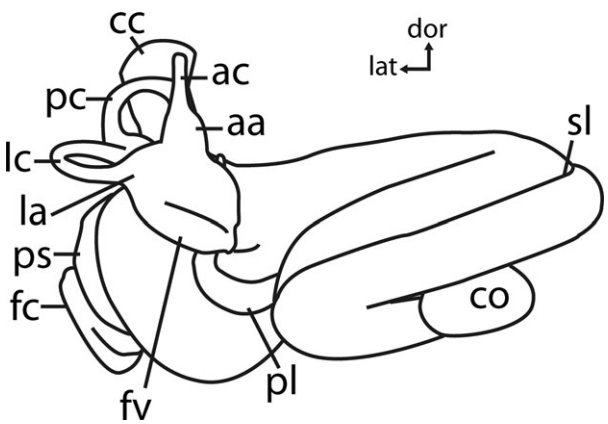

Figure 2. Labeled schematic of the inner ear labyrinths of *Salumiphocaena stocktoni*. Abbreviations listed at the end of the materials and methods section.

Various measurements describing the general morphology of the inner ear labyrinths were taken (Supporting Information, Tables S2–S4), some of which were used in assessing possible hearing frequency ranges. Cochlear spiral length, or basilar membrane length, a proxy sometimes used to infer hearing frequency (West, 1985; Rosowski, 1992), was measured from the start of the laminar gap to the cochlear apex within the cochlea. For comparison with basilar membrane length, surface cochlear spiral length was measured with the cochlea viewed downwards along the axis of rotation. The number of cochlear turns was obtained by counting the number of times the cochlea crossed a line going through the start of the laminar gap through the axis of rotation, and is reported in degrees ('Coil-96' of Ekdale & Rowe, 2011) as well as the number of turns (total degrees divided by 360°) following previously published methods (Ekdale, 2010; Ekdale & Rowe, 2011; Geisler & Luo, 1996). The axial pitch (cochlear height divided by number of turns) and cochlear slope appear to be related to the auditory classifications of extant whales described by Ketten & Wartzok (1990). The product of the length of the cochlear canal and the number of turns is thought to be negatively correlated with hearing, with a smaller product indicating a higher frequency threshold (West, 1985; Manoussaki *et al.*, 2008). The basal ratio, or cochlear aspect ratio, was calculated based on measurements of cochlear spiral height and width. A cochlea is considered 'flattened' if it has an aspect ratio of 0.55 and below, and a high aspect ratio is considered to be above 0.55 (Ekdale, 2010; Gray, 1907, 1908).

Stapedial ratios were obtained when the stapedial footplate was in place, or by using the fenestra vestibuli height divided by perpendicular orthogonal width when the stapes was not preserved. This measurement was used previously as a phylogenetic character differentiating monotremes and marsupials (which have circular fenestra vestibuli) from eutherians (which have elliptical fenestra vestibuli), and was found in cetaceans to be relatively circular compared with other placentals (Ekdale, 2013).

Measurements of the radius at the apex and base of the cochlea, using the line measured through the basilar membrane (after Manoussaki *et al.*, 2008), were obtained to calculate the lower frequency (LF) hearing limit in the extinct porpoises examined in this study (Supporting Information, Table S5). The same measurements also were taken directly on the CT scans as described by Ekdale & Racicot (2015). Manoussaki *et al.* (2008) warned that the formula for predicting the lower end of hearing frequency,

derived from correlations with a number of different mammals, would not be suitable for animals with specialist hearing such as phocoenids, which use narrow-band, high-frequency, echolocation clicks (Morisaka & Connor, 2007). We nonetheless calculated the LF hearing limits based on this equation and report findings for comparison with other studies and as a test of the utility of this method in our sample (Supporting Information, Table S5). Because LF hearing limits are not known currently for many species of odontocetes, hearing frequency ranges based on audiograms or recordings of sound production were obtained from the literature for the six extant species in this study for which such information was available (Table S5). The highest and lowest frequencies from these recorded ranges were investigated as potential correlates with the cochlear radii measurements, but a significant correlation was not found. The known frequency ranges instead were used as comparisons with those calculated using the Manoussaki *et al.* (2008) formula (see above).

Additional measurements of internal structures that may be useful for inferring hearing ranges were taken following previous methods (Fleischer, 1976; Ekdale & Racicot, 2015), including primary and secondary bony lamina widths, laminar gap width (distance between tips of opposing laminae, when preserved), laminar gap 'whole width' (taken in the same orientation as the laminar gap, but extending to the walls of the cochlear spiral as a proxy for laminar gap width, as in many cases the primary and secondary lamina may not be fully preserved axially), diameter of spiral ganglion canal, and thickness of walls separating adjacent whorls of the cochlea (Supporting Information, Table S3).

The relationship of the vestibule and semicircular canals to aquatic agility in cetaceans is not well understood, and has not been considered previously in analyses of agility owing to the derived nature of the anatomy and locomotion of cetaceans relative to terrestrial mammals, except when specifically exploring the inner ear of cetaceans and other aquatic animals (Spoor *et al.*, 2002). We investigated whether ecological or phylogenetic information still could be gleaned from morphological details of the vestibular apparatus in phocoenids, in spite of these marked distinctions. Measurements of the semicircular canals used by previous authors (Spoor *et al.*, 2007; Macrini *et al.*, 2013) to infer locomotor agility in terrestrial animals (i.e. length of the slender portion of the lateral, anterior, and posterior canals; lateral, anterior, and posterior canal heights and widths) were obtained (Supporting Information, Table S4). Radii of curvature were calculated from canal heights and widths using the methods of Spoor *et al.* (2007), i.e., $0.5 \times (\text{canal height} + \text{canal width})/2$, then averaged for comparison. There is a positive correlation between average canal radius and agility of locomotion in primates and other terrestrial mammals, when accounting for body mass and phylogenetic relationships (Spoor *et al.*, 2007).

A method independent of body mass that may be more appropriate for aquatic or extinct animals, for which body mass may be difficult to infer, measures the variance or deviation of ipsilateral (same side) semicircular canal pairs from orthogonality or 90° (90var of Malinzak, Kay & Hullar, 2012, Berlin *et al.* 2013, Ekdale & Racicot, 2015). 90var measurements and calculations were taken following Ekdale & Racicot (2015). Low deviations from 90° indicate a vestibular system that is more sensitive to head rotations, typical of faster moving mammals, while higher deviations indicate less sensitivity to head rotations (Malinzak *et al.* 2012).

Body weights and lengths of extant phocoenid species were compiled from the literature (Silva & Downing, 1995; Supporting Information, Table S2) to determine whether body mass is correlated with some of the measured aspects of the inner ear. When available, the body weights and lengths of the individuals scanned were used, but this was only the case for the two *P. phocoena* specimens and *C. commersonii*. Where individual masses and lengths were not available, the average of the minimum and maximum body weights based on other specimens from that locality (e.g., *Neophocaena phocaenoides*, average of minimum/maximum from South China Sea) and for male and female (*Phocoena dioptrica*), were used. Body lengths of the extinct species can be estimated from other bony anatomy proxies in principle (Pyenson & Sponberg, 2011), but relevant measurements were unavailable to obtain estimates for most specimens. Periotic volume and whole periotic length may be other useful proxies for comparison for the fossil and recent specimens, but not all of these data were available for all individuals analyzed.

Statistical methods

Correlations of measurements among extant species were initially performed using a non-parametric and rank-based statistical test (Spearman's rho), which assesses the degree to which two variables can be described using a monotonic function (Supporting Information, Fig. S1). Aspects of inner ear morphology among extant species that were found to be correlated with body length were subsequently investigated using ordinary least squares (OLS) regression analysis after log10 transformation to extract linear models; these models were subsequently used to estimate the body lengths of extinct

species. Using a similar method, we investigated aspects of cochlear morphology (basilar membrane length and radii ratio, mentioned above) as potential correlates for upper and lower limits of peak or best sensitivity hearing frequencies, but no correlation was found.

Abbreviations

Abbreviations used in the figures are: aa, anterior ampulla; ac, anterior semicircular canal; am, ampulla; ap, anterior process of the periotic/petrosal; cc, canaliculus cochleae; co, cochlea; fc, fenestra cochleae; fv, fenestra vestibuli; la, lateral semicircular canal ampulla; lc, lateral semicircular canal; pbf, posterior bullar facet; pc, posterior semicircular canal; pl, primary lamina; ps, outpocketing for perilymphatic sac; sc, semicircular canal; sl, secondary lamina; st, stapes; vb, vestibule.

RESULTS

Cochlea descriptions

The contribution of the cochlear volume to the whole inner ear labyrinth is near 90% in all of the specimens studied (Supporting Information, Table S2). The lowest percentage contributions were found in extant *Phocoena sinus*, the extant outgroup *Cephalorhynchus commersoni*, and the extinct species *Salumiphocaena stocktoni*, *Haborophocoena toyoshimai* SMAC 1389, *Numataphocoena yamashitai*, and UCMP 128285, ranging from 89–90%; the contributions in the remaining species were 91–95%. No obvious differences in the contribution of the cochlear volume between the left and right digital endocasts are present in recent specimens.

Medial to the canaliculus cochleae, the basal turn continues apically in a straight, diagonal direction rather than having a curved aspect in the recent specimens, with *Neophocaena phocaenoides* having this characteristic developed the least (Figs 3–6 and Supporting Information, S2, S3). This corresponds with a more dorsally directed secondary spiral lamina, and a slight overhang of the cochlear canal proximal to the canaliculus cochleae (Figs 5 and S3). The outgroup *C. commersonii*, and the extinct phocoenids *Numataphocaena yamashitai*, *H. toyoshimai*, *M. nishinoi*, *Pterophocaena nishinoi*, and *S. ceruttii* appear to have a similar shape to *Neophocaena phocaenoides*. This shape difference in extant species having a less round aspect of the cochlear base (and more dorsally directed secondary spiral lamina) is roughly reflected in the basal ratios, in that most extinct species have lower aspect ratio values than do most extant species.

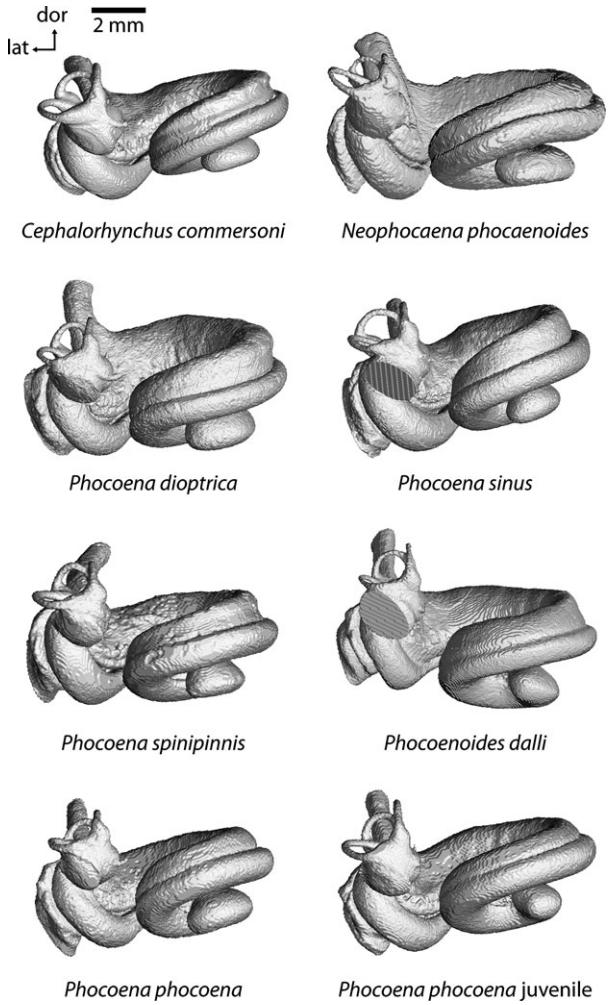

Figure 3. Anterior views of the bony labyrinths of recent specimens examined. For ease of comparison, all specimens are from the right side of the body. Scale bar applies to all specimens.

The canaliculi cochleae for the membranous perilymphatic duct vary in length, width, and orientation among the species studied. The extant *Neophocaena phocaenoides* has the shortest canaliculus cochleae length and it appears the widest in cross-section. In *M. nishinoi*, it appears that some deformation of the canaliculus cochleae region occurred during fossilization, slightly obscuring details of this region (Figs 4, 6 and Supporting Information, S2, S3). In cross-section, the canaliculus cochleae is substantially narrowed dorsally in the extant adult *P. phocoena*, *Phocoena sinus*, and *Phocoena spinipinnis* and in the fossil Phocoenidae cf. UCMP 128285 and *Pterophocaena nishinoi* compared with other specimens (Figs 5–6).

The outpocketing for the perilymphatic sac, and correspondingly the fenestra cochleae, is well

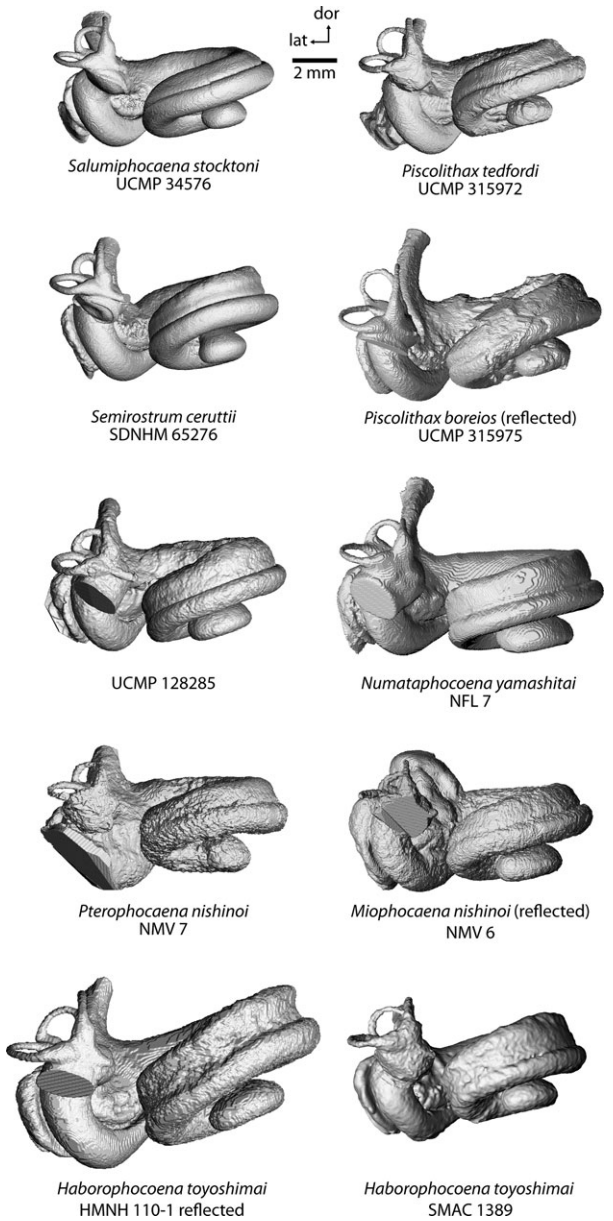

Figure 4. Anterior views of the bony labyrinths of fossil specimens examined. For ease of comparison, all specimens are either from the right side of the body or reflected (as indicated) when from the left side of the body (original orientations shown in Figure S1 of specimens from the left side of the body). Scale bar applies to all specimens.

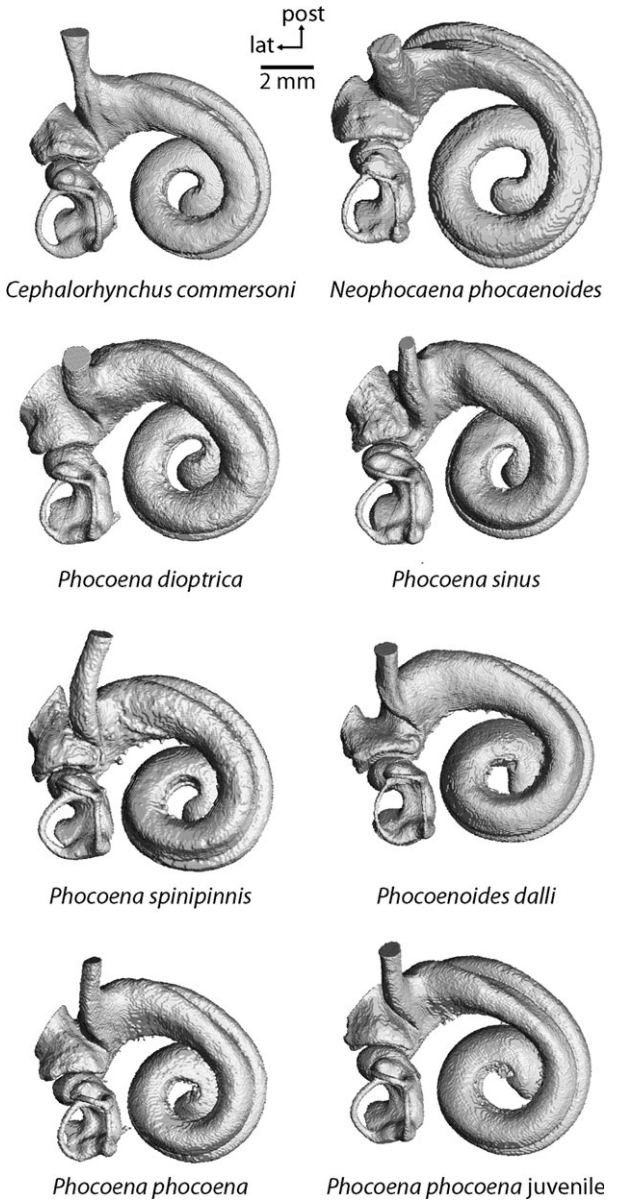

Figure 5. Dorsal views of the bony labyrinths of recent specimens examined. For ease of comparison, all specimens are from the right side of the body. Scale bar applies to all specimens.

separated by a groove (corresponding to a flexure in the bone) from the canaliculus for the cochlear aqueduct in extant *Phocoenoides dalli* (Fig. 5). This condition is not observed in any of the other specimens, although the adult specimens of the extant species *P. phocoena* and *Phocoena sinus* resemble it, with smaller and less obvious separation and orientation of the canaliculus cochleae than in *P. dalli*.

The aspect ratios of cochlear height and width (basal ratio) indicate that most specimens are low-spired, or have 'flattened' cochleae (Supporting Information, Table S2). No obvious outliers are present, and the stem taxon *Salumiphocaena stocktoni* has the lowest basal ratio value (0.37), reflecting its 'flattened' shape. Extinct *P. tedfordi* and *Numataphocoena yamashitai*, and the outgroup taxon *Cephalorhynchus commersoni*, have basal ratio values (0.38–0.39) similar to that of *Salumiphocoena*

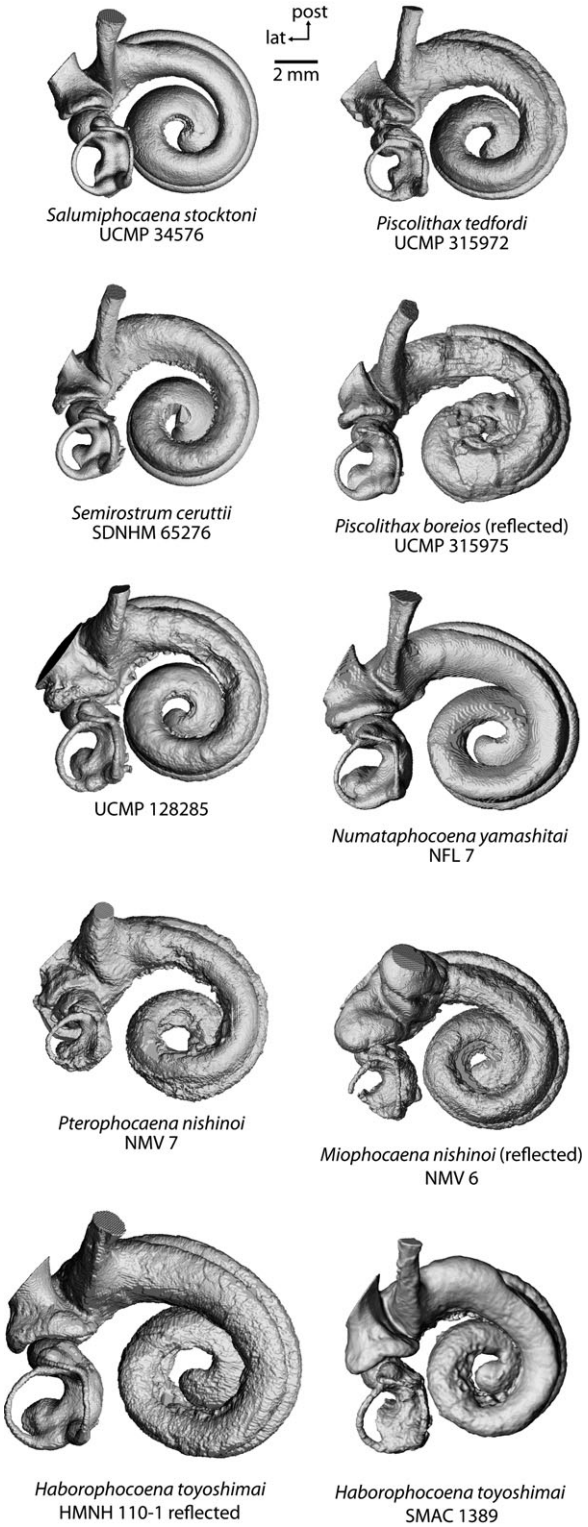

Figure 6. Dorsal views of the bony labyrinths of fossil specimens examined. For ease of comparison, all specimens are either from the right side of the body or reflected (as indicated) when from the left side of the body (original orientations shown in Figure S2 of specimens from the left side of the body). Scale bar applies to all specimens.

stocktoni. The largest aspect ratio is found in the right side of *H. toyoshimai* SMAC 1389 (0.59), indicating less dorsoventral compression than in other specimens, although the left ear of the same individual was calculated as much lower (0.47). Among the fossil specimens, the stem taxa *M. nishinoi* and *S. ceruttii* possess somewhat large basal ratios (0.47 and 0.46, respectively). Among recent specimens, *P. dalli* possesses the largest basal ratio (0.54–0.55). These measurements correspond well with qualitative visual assessment of the cochlear spiral (Fig. 3).

The number of cochlear turns does not vary greatly among specimens examined, and all have fewer than two complete turns (Supporting Information, Table S2). *Phocoenoides dalli* (1.75–1.74), the juvenile *P. phocoena* (1.66), and *Pterophocaena nishinoi* (1.71), possess the fewest number of turns. Similarly, the previously described outgroup *Tursiops truncatus* (Ekdale, 2013; Ekdale & Racicot, 2015) has 1.7 turns, although the number of turns measured and reported in the literature for this animal vary (e.g., 2.25 turns is reported by Ketten, 1997).

The product of the length of the cochlear canal and number of turns (Supporting Information, Table S2) is smallest in the extant outgroup *C. commersonii* (48.44–49.49), and in the extant juvenile *P. phocoena* (45.55–46.54) and *P. dalli* (49.22–49.33). The largest values are found in the extinct species *H. toyoshimai* HMNH 110-1 (85.29), *Numataphocoena yamashitai* (75.52), and UCMP 128285 (68.15). The remaining specimens' measurements vary between 50.59 and 63.67. Among extant species, the largest values are found in *Neophocoena phocaenoides* (61.76–63.67).

Other aspects of the cochlear structure that relate to the auditory types described by Ketten & Wartzok (1990) all are fairly similar in every specimen examined (Supporting Information, Table S2). The smallest values for axial pitch are found in the extant outgroup *C. commersonii* (1.88–1.84) and extant adult *P. phocoena* (2.03–2.20). Fossil specimens with relatively small values are *Salumiphocaena stocktoni* (2.07) and *P. tedfordi* (2.12). Cochlear slope values range from 0.06 to 0.10, with the left ear of the extant outgroup *C. commersonii* and extinct *H. toyoshimai* HMNH 110-1, *Numataphocoena yamashitai, Salumiphocaena stocktoni,* and UCMP 128285 all characterized by the lowest value of 0.06.

The secondary lamina of the outgroup *C. commersonii* appears dorsoventrally wider than in the extant and extinct phocoenids (Fig. 3), instead resembling that in another delphinid outgroup *Tursiops truncatus* (Ekdale, 2013). In all specimens, the secondary spiral laminae extend substantially toward the apex of the cochlea. The remaining dimensions of internal structures of the cochlea do not vary greatly among specimens examined

(Supporting Information, Table S3). The laminar gap widths of the extinct species *Salumiphocaena stocktoni* and *S. ceruttii* are well preserved, and are similar to those of the extant species examined. The measurements at the basal turns of the laminar gaps in these extinct species are closest to those of extant *Phocoena dioptrica*.

Calculations of LF hearing based on the graded ratio are similar among all specimens examined (Supporting Information, Table S5). Some large differences are present between the results based on the Manoussaki *et al.* (2008) method, which uses a projection of the cochlear spiral, vs. the modified method of Ekdale & Racicot (2015), which uses direct measurements from the CT scans. The Manoussaki *et al.* (2008) method resulted in much lower LF estimates than expected in the taxa studied. We expect that the results based on methods described by Ekdale & Racicot (2015) are more accurate because they were measured directly from the CT data rather than adding the step of projecting the cochlear spiral before measuring it, thus we focus our description on those results. The available hearing ranges in the literature do not always include the lowest end of hearing and sound production frequencies, so our ability to compare LF results with known hearing ranges is limited. Substantial differences in values between the sides of each ear are present in extant *Phocoena sinus*, *Phocoena spinipinnis* and extinct *H. toyoshimai*. The majority of phocoenid specimens had higher LF thresholds than extant outgroup delphinid *Tursiops truncatus*, with the exceptions of extant *Phocoena sinus* (right side, 0.19 kHz), and extinct *Haborophocoena nishinoi* SMAC-1389 (right side, 0.17 kHz), *M. nishinoi* (0.15 kHz), and *Salumiphocoena stocktoni* (0.19 kHz). The calculation for the extant adult *P. phocoena* (0.3 kHz) is quite close to the low-frequency threshold documented using physiological audiograms (0.25 kHz, Kastelein, Bunskoek & Hagedoorn, 2002). The extant juvenile *P. phocoena*, however, is calculated as having higher LF thresholds than the adult of the same species (0.48–50 kHz). As expected, the extant outgroup delphinid *C. commersonii* that produces narrow-band high frequency had a similarly high (0.3 kHz) LF threshold to the majority of the phocoenids.

Vestibule descriptions

All of the elliptical recesses of the vestibules bow medially (Figs 5, Supporting Information, S3), similar to the condition in the outgroup delphinid *Tursiops truncatus* and some other placental mammals (Ekdale, 2013). The spherical recess is not distinguishable, because the fenestra vestibuli/stapedial plates make up much of the anterolateral surface of the vestibule in all specimens. The fenestra vestibuli opens out from an anterolateral position in all of the specimens, and the stapedial ratios range from 1.05 to 1.47 (Supporting Information, Table S2), indicating that they are relatively circular compared with other placental mammals, as was found in the cetaceans *Tursiops truncatus* and a balaenopterid fossil described previously (Ekdale, 2013).

Some specimens have more prominent vestibular nerve canals than others. In particular, several branches of the nerve enter the vestibule of *S. ceruttii* just ventral to the anterior and lateral ampullae (Figs 4, 6). Extinct *H. toyoshimai* (all individuals), *M. nishinoi*, *P. boreios*, and UCMP 128285, the extant outgroup *C. commersonii* (which also appears to have two canals, though smaller than *S. ceruttii*), and extant *Phocoena dioptrica* and *P. phocoena* similarly have visible vestibular nerve canals entering the vestibule ventral to the anterior ampullae.

The bony channels for the vestibular aqueducts were not digitally isolated for all specimens, but brief discussion still is warranted. As in previously described cetaceans (e.g., Ekdale, 2013), this canal is thin and thread-like until it begins to open out to the endocranial aperture in all specimens studied. Variation in the widths of the endocranial opening is apparent among different species, and may require further investigation as potential phylogenetic characters.

As in previously described cetaceans (Ekdale, 2013), the posterior limbs of the lateral canals empty into the posterior ampullae immediately anterior, or slightly lateral and dorsal, to the vestibular aperture of the ampulla. Lateral and anterior ampullae are well separated, and a common crus is present in each specimen (Figs 3–6, Supporting Information, S2, S3).

Semicircular canal arc radii averages ranged from 0.55 to 0.56 in the extant adult *P. phocoena* and 1.14 in the extinct *H. toyoshimai* HMNH 110-1 (Supporting Information, Table S4). The average canal arc radii are generally greater in the fossil specimens examined (0.57–1.14), although some fall within the range of extant species (0.55–0.74). Measurements of fossil specimens that fall within the range of recent specimens comprise *M. nishinoi* (0.57), *Pterophocaena nishinoi* (0.63), and *S. ceruttii* (0.72). Accounting for correlations with body size may be appropriate for further investigation of the ecological or other vestibular acuity significance of these measurements.

The lengths of the slender portions of the semicircular canals vary among the specimens examined. The absolute lengths of the lateral canals are generally the longest among all specimens examined, while the posterior canals are generally the shortest (Supporting Information, Table S4). One exception is in the extant

P. dalli, which has shorter (1.91–2.21 mm) lateral canals than anterior canals (2.06–2.29 mm).

Calculations of 90var (semicircular canal deviations from 90°, Supporting Information, Table S4) range from 12.7 (right side of *P. dalli*) to 25.4 (left side of adult *P. phocoena*), which are generally greater than in other mammals (2.28–15.45 as reported by Berlin *et al.* 2013). Substantial variation between left and right sides is present in *Phocoena sinus* (12.73 and 20.20, respectively). Lower values in both the left and right ears of the recent sample are found in *Phocoena dioptrica* (17.97 and 18.1, respectively) and *P. dalli* (15.4 and 12.7, respectively), implying greater sensitivity to head rotations in these species. These results coincide with the offshore habitat preferences and corresponding skull morphology (alignment of the foramen magnum with the vertebral column, less ventral inclination of the rostrum, and larger and more concave facial region) described for *Phocoena dioptrica* and *P. dalli* (Barnes, 1985; Brownell & Clapham, 1999b; Houck & Jefferson, 1999; Read, 2002; Galatius *et al.*, 2011). The remaining extant porpoise species have 90var values indicating vestibular systems consistent with less sensitivity to head rotations and prefer near-shore, coastal, or even riverine habitats in the case of some *Neophocaena phocaenoides* populations (Brownell & Clapham, 1999a; Kasuya, 1999; Read, 1999, 2002; Vidal, Brownell & Findley, 1999).

Statistical correlations with body length in extant species

None of the inner ear labyrinth measurements were found to correlate with known body weights in extant species; several measurements, however, correlate with body length. Lateral semicircular canal height (Sp. rho = 0.5, $P < 0.05$) and volume measurements of the entire/whole labyrinth (Sp. rho = 0.81, $P < 0.001$), cochlear volume (Sp. rho = 0.81, $P < 0.001$), cochlear surface area (Sp. rho = 0.71, $P < 0.01$), cochlear spiral surface length (Sp. rho = 0.75, $P < 0.001$), and basilar membrane length (Sp. rho = 0.69, $P < 0.01$) were all positively correlated with body length (Supporting Information, Fig. S1). Correspondingly, no vestibular measurement (including those of the semicircular canals) correlated with cochlear measurements, except the semicircular canal arc radius of curvature measurements with cochlear coil measurements.

Body length predictions

Among inner ear measurements that showed strong (rank-based) correlation with body length (lateral semicircular canal height, whole labyrinth volume, cochlear spiral length, cochlear spiral length taken on surface, cochlea volume, and cochlear surface area), whole labyrinth volume showed the best linear fit after log10 transformation ($R^2 = 0.62$, $P < 0.001$). This measurement is convenient as a possible body length correlate and proxy, as it is easily extracted from CT scans. The covariance model can be written as:

$$\log10\,(\text{body length}) = 1.3713 \times \log10\,(\text{labyrinth volume}) - 0.4885.$$

This model was used to predict the body lengths of extant species, and the resulting differences between observed and predicted body lengths used to calculate percent prediction errors (PPEs) for each extant species. The linear model then was used to estimate the body lengths of extinct porpoises, and uncertainty around these estimates calculated using the mean PPE calculated for all extant taxa (12.23%). The results illustrate that of the 11 fossil specimens treated in this analysis, four (*P. boreios*, *P. tedfordi*, *Salumiphocaena stocktoni*, and *S. ceruttii*) have estimated body lengths that fall within the broad range of extant species (~100–250 cm; Fig. 7). In contrast, two extinct species (*Numataphocoena yamashitai*, and *H. toyoshimai* HMNH 110-1) have estimated body lengths that are significantly larger than any observed in an extant species; *H. toyoshimai* in particular might have been extremely large for a phocoenid (~700 cm in length). The left and right labyrinths of *H. toyoshimai* SMAC 1289 indicate that its body length was larger than extant or some other extinct species (~260–280 cm), but not quite as large as the other *H. toyoshimai* sample. The remaining fossil specimens examined range in predicted lengths from ~275–290 cm. Given that the labyrinth volume of *M. nishinoi* is likely lower than it would be if parts of the vestibule had been completely preserved, the prediction for its body length probably is a slight underestimate.

DISCUSSION

Similarities among dimensions of the cochleae in the specimens analyzed provide insight into the evolution of phocoenids and the probable hearing capabilities of extinct and rare extant species. The basal ratio of the cochlea in the specimens studied does not vary greatly. *Salumiphocaena stocktoni*, the arguably earliest (Miocene Monterey Formation 9–12.6 Ma) described stem phocoenid in this study possessed a low-spired cochlea, similar to early-diverging extant phocoenids and the ecologically similar delphinid species *C. commersonii* (which we would

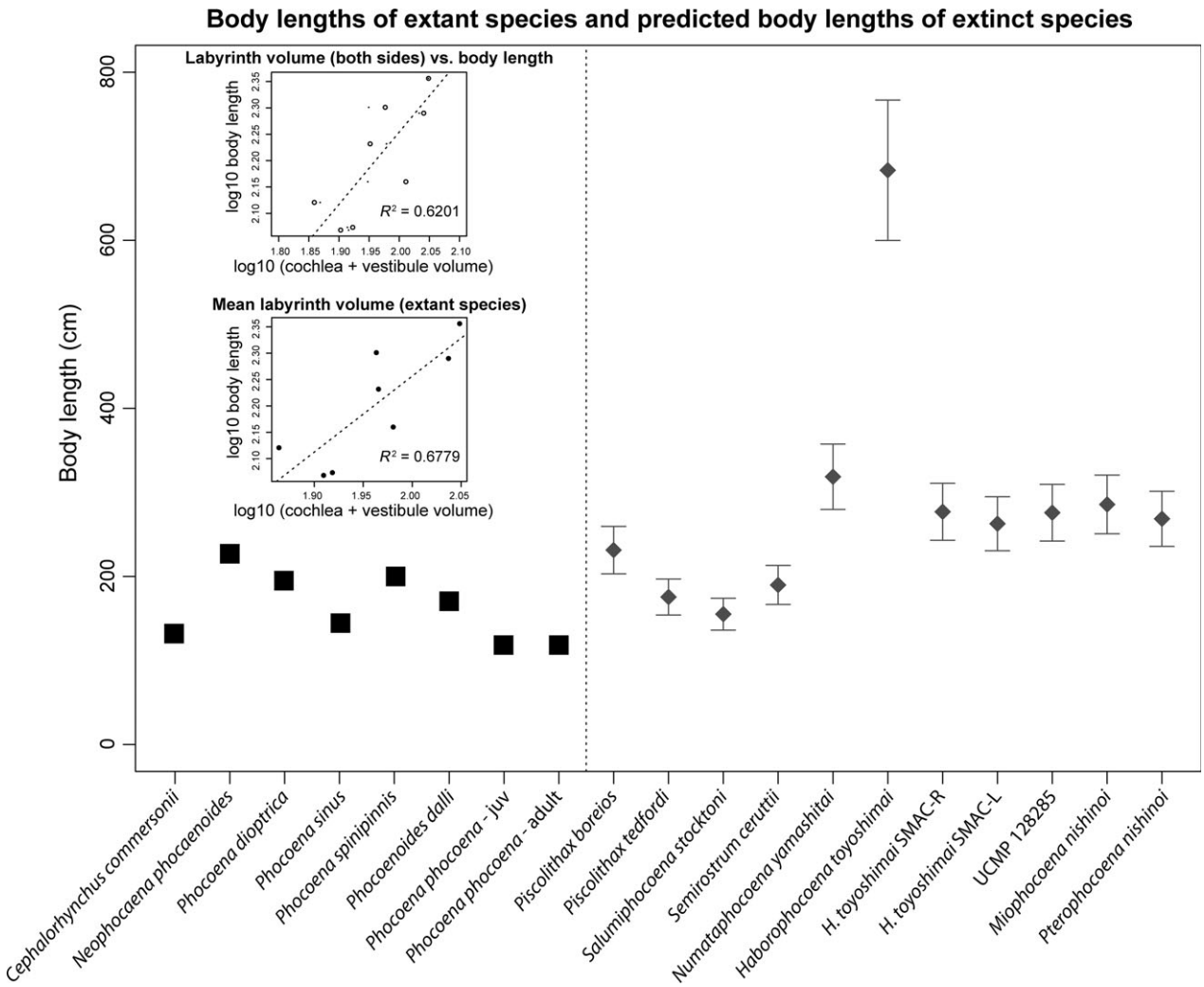

Figure 7. Extant porpoise and dolphin body lengths (squares) and body length predictions of extinct porpoises (diamonds with bracketing percent prediction errors). Inset represents the regressions used for the prediction model.

expect to be similar). *Pterophocaena nishinoi*, although geologically younger (9.2–9.3 Mya), is purportedly the earliest-diverging described porpoise (Murakami *et al.* 2012). The basal ratio of *Pterophocaena nishinoi* indicates less 'flattening' than in *Salumiphocaena stocktoni*, but still falls within the range of extant species. The later-diverging extant species *P. dalli* having the highest-spired cochlea may be an autapomorphy for the species. This is further supported by *P. dalli* having the fewest cochlear turns among extant adult species studied. Comparisons with additional delphinids and at least one other outgroup, such as a monodontid, would be necessary to determine whether the delphinid/phocoenid common ancestor also had a low-spired cochlea to the degree reported here. Nonetheless, other cetaceans (including *Tursiops truncatus*, an outgroup delphinid without specialized hearing and sound production) have been described as low-spired relative to other mammals (Ekdale, 2013; Ekdale & Racicot, 2015), and are within a similar range (albeit somewhat higher, 0.5–0.7) of basal ratio values as those reported here. Our calculated basal ratio values are notably larger than those reported for *P. phocoena* by Ketten & Wartzok (1990), but are still generally below or close to 0.55.

Further metrics describing cochlear structure that may be related to hearing frequency suggest roughly similar hearing ranges in all specimens examined. The range of values for axial pitch and cochlear slope for all specimens are consistent among specimens examined, although the values are higher than expected for 'type I' spirals of Ketten & Wartzok (1990); peak energy echolocation clicks of known

species with this spiral type are above 100 kHz. Internal dimensions of the cochlea, however, reflect expected measurements for 'type I' species, in particular in the similar dimensions of the laminar gap width and whole laminar gap width along the length of the cochlea in *Salumiphocaena stocktoni* and *Semirostrum cerutti*. Taken together with the calculations of LF hearing based on the graded ratio (Supporting Information, Table S5), our results suggest that extinct phocoenids had similar hearing ranges to extant species. This implies that narrow-band high-frequency sound production and hearing evolved early in the history of this group, at the latest between 7–10 Ma. The early evolution of high-frequency hearing may indicate that ecological pressures and drivers, such as avoiding large predators (Anderson & Amundin, 1976; Madsen *et al.*, 2005; Morisaka & Connor, 2007), impacted early phocoenids and caused them to occupy an acoustic niche space that continues to today.

Some features of the cochlea in the specimens studied may be useful as phylogenetic characters in future analyses. *Phocoenoides dalli* in particular possesses a number of potential autapomorphies, such as the groove expressed on the endocast of the cochlear canal between the fenestra cochleae and the canaliculus cochleae. A potential synapomorphy observed in the majority of the later-diverging extant phocoenids (*Phocoena dioptrica*, *Phocoena sinus*, *P. dalli*, and *P. phocoena*) includes the diagonal aspect of the dorsal surface of the basal turn of the cochlea, although *C. commersonii* has a similar morphology, possibly indicating a functional correspondence related to similar hearing frequency range. Variation in length, orientation, and cross-sectional shape of the canaliculus cochleae also may represent phylogenetically informative characters.

Morphometrics of the skull and postcranial skeleton in extant phocoenids show interspecific differences relating to habitat preference resulting from progenetic paedomorphosis (Galatius *et al.*, 2011). Larger adult body sizes, less pronounced paedomorphic characteristics, and the foramen magnum/occipital condyles and rostrum aligning more with the vertebral column are found in the two species that prefer pelagic habitats (Galatius *et al.*, 2011). The alignment of the rostrum and foramen magnum/occipital condyles with the vertebral column is thought to be related to pelagic feeding, whereas ventral inclination of the rostrum in the coastal species may facilitate scanning of riverbeds and other shallow waters (Monteiro-Filho, Monteiro & dos Reis, 2002; Galatius *et al.*, 2011). Another study showed that the optic tracts are more laterally oriented in pelagic-preferring species than coastal species, which have optic tracts that are directed more anteriorly (Racicot & Colbert, 2013), both of which may impact visual acuity for different ecologies. An intriguing result from the analyses of the semicircular canal measurements in this study is that species described as preferring pelagic or offshore habitats, *Phocoena dioptrica* and *P. dalli*, possess lower 90var values (indicating a vestibular system that is more sensitive to head rotations, and mean angular velocities of the head are higher) than those that are considered coastal species (*P. phocoena*, *Phocoena sinus*, *Phocoena spinipinnis*, and *Neophocaena phocaenoides*). Comparatively reduced sensitivity to head rotations in species that prefer coastal habitats may be important in the slower moving process of scanning their environment and/or searching for prey. Pelagic species, by contrast, may more regularly employ faster swimming and quicker prey-capture. *Phocoenoides dalli* are thought to be the fastest swimmers among small cetaceans, and they regularly bow ride (Reeves *et al.*, 2002), which lends support to this hypothesis. Little information is known about the biology of *Phocoena dioptrica*, but our results would suggest the ability to employ active and fast swimming movement.

Extinct species with 90var results that fall within the ranges of more pelagic extant phocoenid species include *H. toyoshimai*, *P. tedfordi*, *Pterophocaena nishinoi*, *M. nishinoi*, and *Salumiphocaena stocktoni*. The remaining extinct species (*N. yamashitai*, *P. boreios*, *S. ceruttii*, and UCMP 128285) fall into similar 90var ranges to the extant species that prefer coastal areas. Fossil locality data (although we acknowledge that this is more speculative, as carcasses can float, and potentially move long distances from their preferred habitats) and inferences based on skeletal and skull morphology in most instances further support the interpretations of preference for coastal or pelagic habitats in the extinct species. For example, the Monterey Formation, from which *Salumiphocaena stocktoni* was recovered, is a pelagic to hemipelagic (marginal marine) depositional environment (Barnes, 1977; Isaacs, 2001). *Semirostrum cerutti* was deposited in the near-shore San Diego Formation (Deméré, 1983; Boessenecker, 2013; Racicot *et al.*, 2014) and is interpreted to have preferred a coastal habitat crucial for its unique feeding ecology (Racicot & Rowe, 2014; Racicot *et al.*, 2014). An interesting exception is the two *Piscolithax* species, which were both found in the coastal indeterminate Almejas Formation (Barnes, 1984; Boessenecker, 2013), indicating that they were occupying different niche spaces (although not concurrently, as *P. boreios* was found in a geologically younger section of the Almejas Formation). Further support for this is the elevated vertex and more dorsal positioning of the foramen magnum in *P. tedfordi* (Barnes, 1984), as in extant species that prefer pelagic habitats (Galatius *et al.*, 2011), and the lower

positioning of the vertex in *P. boreios* (Barnes, 1984), which is similar to extant species that prefer coastal habitats. Our results therefore suggest that inferences can be made about the ecologies of extinct porpoises, and possibly other cetaceans, even when only the petrosal or periotic is preserved. To test whether habitat preference can be inferred using 90var results, additional comparative studies should be done with different cetacean groups. If correlations can be made with average swimming speeds or some other known measurements for extant cetaceans, reconstructing habitat preference and locomotory abilities in extinct cetaceans can be done with more confidence.

Correlation of body size with inner ear labyrinth measurements is expected (e.g., Ekdale, 2013), but in this study only a positive correlation with body length and not with body weight was found. The lack of correspondence with body weight was not unexpected because body mass in fully aquatic mammals is not necessarily constrained in the same ways as in terrestrial mammals (Clauset, 2013); the sample size also may have been too small to document a close relationship with widely varying individual body weights. Correlation of body length with certain bony labyrinth measurements implies that metrics (lateral semicircular canal height, whole labyrinth volume, cochlear spiral length, cochlear spiral length taken on surface, cochlea volume, and cochlear surface area; Supporting Information, Fig. S1), particularly of the cochlea, are dependent on body size (with body length as a proxy). Lengths and weights of marine mammal fossils are often difficult to estimate due to lack of adequate measurement data. Therefore, the general lack of correlation between vestibular measurements and cochlear measurements implies that one could be used for standardization of the other for comparative purposes. Further, the decoupling of the relationship between the cochlea and vestibule in most measured features may have direct implications for inferences of both auditory and locomotor functions that should be explored further.

The correlation between anterior and posterior semicircular canal arc radii of curvature and the degree of cochlear coiling/number of turns in extant species is an unexpected result. The relationship between semicircular canals and cochlear coiling may be a developmental or allometric relationship related to a corresponding increase or decrease in size of these regions. Alternatively, a functional correspondence also may be considered in a possible connection between biosonar and vestibular acuity (i.e., importance of hearing expressed in number of turns for interpreting their three-dimensional environment).

The body length predictions presented are a reasonable first step in estimating body length in extinct porpoise species, which also could help with future estimations of body length in other fully aquatic mammals. Body size and length typically are difficult to estimate for extinct species consisting of fragmentary specimens, but this example works toward enhanced understanding of several aspects of cetacean biology, especially from the fossil record where isolated tympanoperiotics sometimes provide the only preserved biological data. The extremely large body size predicted for the stem phocoenid *H. toyoshimai* indicates that it may have retained an ancestrally large body size similar to extant monodontids (the sister group of phocoenids in molecular analyses, e.g., McGowen, Spaulding & Gatesy, 2009) such as the beluga. Given that the other individual of *H. toyoshimai* was predicted as within a range closer to the other extinct and extant phocoenids, there may have been large differences in adult and younger individual body sizes within *Haborophocoena*. Ichishima & Kimura (2013) suggested that, based on the overall smaller skull size and other features, SMAC 1389 was probably a younger individual than the type specimen of *Haborophocoena* (HMNH 110-1). Ichishima & Kimura (2013) also noted that the slightly smaller size of SMAC 1389 periotics were still within the range of expected interspecific variation, and that odontocete ear bones, as in other mammals, do not substantially increase in size postnatally. The overall larger body sizes predicted for most of the extinct species, which are primarily the phylogenetically earlier diverging species, may indicate that the extinct phocoenids examined had not yet evolved the paedomorphic characteristics documented in extant species. The results of this study suggest that body length predictions can be enhanced and further explored among other extant aquatic mammal groups, to reliably infer body sizes in those clades of fossil specimens that consist of fragmentary material.

In summary, a comprehensive dataset comprising digital endocasts of the inner ear labyrinths derived from CT scans of all known extant and many extinct phocoenids, along with an ecologically similar delphinid relative, provides insight into the evolution and ecology of this diverse cetacean group. We show that high-frequency hearing at the level observed in extant phocoenids was present in the earliest known extinct phocoenids, by approximately 11 million years ago. Further, habitat preference and ecologies, or at least whether a species was faster or slower swimming, is possible to infer in extinct species based on measurements of the vestibule. We find that lower 90var values, indicating faster moving animals, were present in the extant porpoise species that prefer pelagic habitats, while higher values are found in species that prefer coastal habitats. Extending these results to extinct species finds support in other skeletal attributes and possibly geological formation. Finally,

correlations with inner ear labyrinth volume and total body length were used to obtain a predictive equation to estimate body size in extant and extinct phocoenids, although this should be explored in more detail in future studies. The extensive detailed data from this work will prove useful when incorporated into phylogenetic datasets and on their own in understanding more about the biology of extinct and rare extant phocoenid species, highlighting the wealth of morphological and physiological information that digital endocasts of inner ear labyrinths provide.

ACKNOWLEDGEMENTS

Scans were funded in part by a Yale Institute for Biospheric Studies Dissertation Enhancement Grant, AMNH Lerner–Gray Fund for Marine Research, and NSF-East Asia Pacific Summer Institute grant to RAR, who is presently funded by NSF (grants DEB 1331980 and PLR 134175). We thank museums and staff for access to specimens and loaning specimens for CT scanning: T. Deméré and K. Randall (SDNHM); K. Helgen and C. Potter (NMNH); C. Conroy (MVZ, Berkeley); M. Flannery (CAS); P. Holroyd (UCMP); N.R.P. Gooddall (AMMA); R. Pittman and W. Perrin (Southwest Fisheries Science Center); E. Westwig and N. Duncan (AMNH); T. K. Yamada, Y. Tajima, N. Kurihara (NMNS); Y. Hikida (NMV); S. Yamashita (NFM); H. Furusawa (SMAC); Y. Okazaki and H. Ohashi (KMNH); and H. Sawamura (AMP). The authors thank M. Colbert and J. Maisano at the University of Texas High-Resolution X-Ray CT facility, J. Thostensen and M. Hill of the AMNH MIF, and C. Sakata of the National Museum of Nature and Science, Tokyo, for CT scanning specimens for this study. We gratefully acknowledge the helpful comments of the reviewers (Drs. Maeva Orliac, Eric Ekdale, and Robert W. Boessenecker), which significantly improved the final version of this manuscript.

REFERENCES

Anderson SH, Amundin M. 1976. Possible predator-related adaptation of sound production and hearing in the harbour porpoise (*Phocoena phocoena*). *Aquatic Mammals* **4:** 56–58.

Barnes LG. 1977. Outline of eastern North Pacific fossil cetacean assemblages. *Systematic Zoology* **25:** 321–343.

Barnes LG. 1984. Fossil odontocetes (Mammalia: Cetacea) from the Almejas Formation, Isla Cedros, Mexico. *Paleobios* **42:** 1–46.

Barnes LG. 1985. Evolution, taxonomy and antitropical distributions of the porpoises (Phocoenidae, Mammalia). *Marine Mammal Science* **1:** 149–165.

Berlin JC, Kirk EC, Rowe TB. 2013. Functional implications of ubiquitous semicircular canal non-orthogonality in mammals. *PLoS One* **8:** e79585.

Boessenecker RW. 2013. A new marine vertebrate assemblage from the Late Neogene Purisima Formation in central California, Part II: pinnipeds and cetaceans. *Geodiversitas* **35:** 815–940.

Brownell RL, Clapham PJ. 1999a. Burmeister's porpoise – *Phocoena spinipinnis* Burmeister 1865. In: Ridgway SH, Harrison SR, eds. *Handbook of Marine Mammals: The Second Book of Dolphins and the Porpoises*. San Diego: Academic Press, 393–428.

Brownell RL, Clapham PJ. 1999b. Spectacled porpoise – *Phocoena dioptrica* Lahille 1912. In: Ridgway SH, Harrison SR, eds. *Handbook of Marine Mammals: The Second Book of Dolphins and Porpoises*. San Diego: Academic Press, 379–392.

Clauset A. 2013. How large should whales be? *PLoS ONE* **8:** e53967.

Cranford TW, Krysl P, Amundin M. 2010. A new acoustic portal into the odontocete ear and vibrational analysis of the tympanoperiotic complex. *PLoS ONE* **5:** e11927.

Deméré TA. 1983. The Neogene San Diego basin: a review of the marine Pliocene San Diego formation. In: Larue DK, Steel RJ, eds. *Cenozoic marine sedimentation, Pacific margin, USA*. Los Angeles, CA: Society of Economic Paleontologists and Mineralogists, 187–195.

Ekdale E. 2010. Ontogenetic variation in the bony labyrinth of *Monodelphis domestica* (Mamammila: Marsupialia) following ossification of the inner ear cavities. *Anatomical Record* **293:** 1896–1912.

Ekdale EG. 2013. Comparative anatomy of the bony labyrinth (inner ear) of placental mammals. *PLoS ONE* **8:** e66624.

Ekdale EG, Racicot RA. 2015. Anatomical evidence for low frequency sensitivity in the inner ear of *Zygorhiza kochii* (Cetacea, Basilosauridae). *Journal of Anatomy* **226:** 22–39.

Ekdale EG, Rowe T. 2011. Morphology and variation within the bony labyrinth of zhelestids (Mammalia: Eutheria) and other therian mammals. *Journal of Vertebrate Paleontology* **31:** 658–675.

Fleischer G. 1976. Hearing in extinct cetaceans as determined by cochlear structure. *Journal of Paleontology* **50:** 133–152.

Galatius A. 2010. Paedomorphosis in two small species of toothed whales (Odontoceti): how and why? *Biological Journal of the Linnean Society* **99:** 278–295.

Galatius A, Berta A, Frandsen MS, Goodall RNP. 2011. Interspecific variation of ontogeny and skull shape among porpoises (Phocoenidae). *Journal of Morphology* **272:** 136–148.

Geisler JH, Luo Z. 1996. The petrosal and inner ear of *Herpetocetus* sp. (Mammalia: Cetacea) and their implications for the phylogeny and hearing of archaic mysticetes. *Journal of Paleontology* **70:** 1045–1066.

Gray AA. 1907. *The labyrinth of animals: including mammals, birds, reptiles, and amphibians*. London: J. and A. Churchill.

Gray AA. 1908. *The labyrinth of animals: including mammals, birds, reptiles and amphibians*. London: J. and A. Churchill.

Grohé C, Tseng ZJ, Lebrun R, Boistel R, Flynn JJ. 2015. Bony labyrinth shape variation in extant Carnivora: a case study of Musteloidea. *Journal of Anatomy*. **228:** 366–383.

Gutstein CS, Figueroa-Bravo CP, Pyenson ND, Yury-Yañez RE, Cozzuol MA, Canals M. 2014. High frequency echolocation, ear morphology, and the marine-freshwater transition: a comparative study of extant and extinct toothed whales. *Palaeogeography, Palaeoclimatology, Palaeoecology* **400:** 62–74.

Houck WJ, Jefferson TA. 1999. Dall's porpoise–*Phocoenoides dalli*. In: Ridgway SH, Harrison SR, eds. *Handbook of marine mammals: the second book of Dolphins and the Porpoises*. San Diego: Academic Press, 443–472.

Houser DS, Moore PW, Johnson S, Lutmerding B, Branstetter B, Ridgway S. 2010. Relationship of blood flow and metabolism to acoustic processing centers of the dolphin brain. *Acoustical Society of America* **128:** 1460–1466.

Ichishima H, Kimura M. 2013. New material of *Haborophocoena toyoshimai* (Odontoceti: Phocoenidae) from the Lower Pliocene Embetsu Formation of Hokkaido, Japan. *Paleontological Research* **17:** 127–137.

Isaacs CM. 2001. Depositional framework of the Monterey Formation, California. In: Isaacs CM, Rullkotter J, eds. *The monterey formation – from rocks to molecules*. New York: Columbia University Press, 1–30.

Kasuya T. 1999. Finless porpoise–*Neophocaena phocoenoides* (G. Cuvier, 1829). In: Ridgway SH, Harrison SR, eds. *Handbook of marine mammals: the second book of Dolphins and the Porpoises*. San Diego: Academic Press, 411–442.

Kastelein RA, Bunskoek P, Hagedoorn M. 2002. Audiogram of a harbor porpoise (*Phocoena phocoena*) measured with narrow-band frequency-modulated signals. *Journal of the Acoustical Society of America* **208:** 181–194.

Ketten DR. 1997. Structure and function in whale ears. *Bioacoustics* **8:** 103–135.

Ketten DR, Wartzok D. 1990. Three-dimensional reconstructions of the dolphin ear. In: Thomas J, Kastelein R, eds. *Sensory abilities of cetaceans*. New York: Plenum, 81–105.

Kyhn LA, Jensen FH, Beedholm K, Tougaard J, Hansen M, Madsen PT. 2010. Echolocation in sympatric Peale's dolphins (*Lagenorhynchus australis*) and Commerson's dolphins (*Cephalorhynchus commersonii*) producing narrow-band high-frequency clicks. *Journal of Experimental Biology* **213:** 1940–1949.

Luo Z, Eastman ER. 1995. Petrosal and inner ear of a squalodontoid whale: implications for evolution of hearing in odontocetes. *Journal of Vertebrate Paleontology* **15:** 431–442.

Luo Z, Marsh K. 1996. The petrosal (periotic) and inner ear structure of a Pliocene kogiine whale (Odontoceti, Mammalia): implications on relationships and hearing evolution of toothed whales. *Journal of Vertebrate Paleontology* **16:** 328–348.

Macrini TE, Flynn JJ, Croft DA, Wyss AR. 2010. Inner ear of a notoungulate placental mammal: anatomical description and examination of potentially phylogenetically informative characters. *Journal of Anatomy* **216:** 600–610.

Macrini TE, Flynn JJ, Ni X, Croft DA, Wyss AR. 2013. Comparative study of notoungulate (Placentalia, Mammalia) bony labyrinths and new phylogenetically informative inner ear characters. *Journal of Anatomy* **223:** 442–461.

Madsen PT, Carder DA, Beedholm K, Ridgway SH. 2005. Porpoise clicks from a sperm whale nose – convergent evolution of 130 kHz pulses in toothed whale sonars? *Bioacoustics* **15:** 195–206.

Malinzak MD, Kay RF, Hullar TE. 2012. Locomotor head movements and semicircular canal morphology in primates. *Proceedings of the National Academy of Sciences of the United States of America*, **109:** 17914–17919.

Manoussaki D, Chadwick RS, Ketten DR, Arruda J, Dimitriadis EK, O'Malley JT. 2008. The influence of cochlear shape on low-frequency hearing. *Proceedings of the National Academy of Sciences of the United States of America* **105:** 6162–6166.

McGowen MR, Spaulding M, Gatesy J. 2009. Divergence date estimation and a comprehensive molecular tree of extant cetaceans. *Molecular Phylogenetics and Evolution* **53:** 891–906.

Miller LA, Wahlberg M. 2013. Echolocation by the harbor porpoise: life in coastal waters. *Frontiers in Physiology* **4:** 1–6.

Monteiro-Filho ELD, Monteiro LR, dos Reis SF. 2002. Skull shape and size divergence in dolphins of the genus *Sotalia*: a tridimensional morphometric analysis. *Journal of Mammalogy* **83:** 125–134.

Mooney TA, Yamato M, Branstetter BK. 2012. Hearing in cetaceans: from natural history to experimental biology. *Advances in Marine Biology* **63:** 197–246.

Morell M, Degollada E, van der Schaar M, Alonso JM, Delory E, López A, Dewez A, André M. 2007. Comparative morphometry of odontocete ears through computerized tomography. *Journal of the Marine Biological Association of the United Kingdom* **87:** 69–76.

Morisaka T, Connor RC. 2007. Predation by killer whales (*Orcinus orca*) and the evolution of whistle loss and narrow-band high frequency clicks in odontocetes. *Journal of Evolutionary Biology* **20:** 1439–1458.

Murakami M, Shimada C, Hikida Y, Hirano H. 2012a. A new basal porpoise, *Pterophocaena nishinoi* (Cetacea, Odontoceti, Delphinoidea), from the upper Miocene of Japan and its phylogenetic relationships. *Journal of Vertebrate Paleontology* **32:** 1157–1171.

Murakami M, Shimada C, Hikida Y, Hirano H. 2012b. Two new extinct basal phocoenids (Cetacea, Odontoceti, Delphinoidea), from the upper Miocene Koetoi Formation of Japan and their phylogenetic significance. *Journal of Vertebrate Paleontology* **32:** 1172–1185.

Murakami M, Shimada C, Hikida Y, Hirano H. 2015. New small phocoenid from the Pliocene of Hokkaido, northern Japan: insight into the growth rate and vertebral evolution of porpoises. *Acta Palaeontologica Polonica* **60:** 97–111.

Ni X, Flynn JJ, Wyss AR. 2010. The bony labyrinth of the early platyrrhine primate Chilecebus. *Journal of Human Evolution* **59:** 595–607.

Park T, Fitzgerald EMG, Evans AR. 2016. Ultrasonic hearing and echolocation in the earliest toothed whales. *Biology Letters* **12:** 20160060.

Parks SE, Ketten DR, O'Malley JT, Arruda J. 2007. Anatomical predictions of hearing in the North Atlantic Right Whale. *The Anatomical Record* **290:** 734–744.

Pyenson ND, Sponberg SN. 2011. Reconstructing body size in extinct crown cetacea (Neoceti) using allometry, phylogenetic methods, and tests from the fossil record. *Journal of Mammalian Evolution* **18:** 269–288.

Racicot RA, Colbert MW. 2013. Morphology and variation in porpoise (Cetacea: Phocoenidae) cranial endocasts. *The Anatomical Record* **296:** 979–992.

Racicot RA, Rowe T. 2014. Endocranial anatomy of a new fossil porpoise (Odontoceti: Phocoenidae). *Journal of Paleontology* **88:** 652–663.

Racicot RA, Demere TA, Beatty BL, Boessenecker RW. 2014. Unique feeding morphology in a new prognathus extinct porpoise from the Pliocene of California. *Current Biology* **24:** 774–779.

Read AJ. 1999. Harbour porpoise *Phocoena phocoena* (Linnaeus, 1758). In: Ridgway SH, Harrison SR, eds. *Handbook of marine mammals: the second book of Dolphins and the Porpoises*. San Diego: Academic Press, 323–355.

Read AJ. 2002. Porpoises, overview. In: Perrin WF, Würsig B, Thewissen JGM, eds. *Encyclopedia of marine mammals*. San Diego: Academic Press, 982–985.

Reeves RR, Stewart BS, Clapham PJ, Powell JA. 2002. *Guide to marine mammals of the world*. New York, NY: Alfred A. Knopf Inc.

Rosowski JJ. 1992. Hearing in transitional mammals: predictions from the middle-ear anatomy and hearing capabilities of extant mammals. In: Webster DB, Popper AN, Fay RR, eds. *The evolutionary biology of hearing*. New York, New York: Springer, 615–631.

Sensor JD, Suydam R, George JC, Liberman MC, Lovano D, Rhaganti MA, Usip S, Vinyard CJ, Thewissen JGM. 2015. The spiral ganglion and Rosenthal's canal in beluga whales. *Journal of Morphology* **276:** 1455–1466.

Silva M, Downing JA. 1995. *CRC Handbook of mammalian body masses*. New York: CRC Press.

Spoor F, Bajpai S, Hussain ST, Kumar K, Thewissen JGM. 2002. Vestibular evidence for the evolution of aquatic behaviour in early cetaceans. *Nature* **417:** 163–166.

Spoor F, Garland T, Krovitz G, Ryan TM, Silcox MT, Walker A. 2007. The primate semicircular canal system and locomotion. *Proceedings of the National Academy of Sciences of the United States of America* **104:** 10808–10812.

Vidal O, Brownell RL, Findley LT. 1999. Vaquita *Phocoena sinus* Norris and McFarland, 1958. In: Ridgway SH, Harrison SR, eds. *Handbook of marine mammals. The second book of Dolphins and the Porpoises*. San Diego, CA: Academic Press, 357–378.

West CD. 1985. The relationship of the spiral turns of the cochlea and the length of the basilar membrane to the range of audible frequencies in ground dwelling mammals. *Journal of the Acoustical Society of America* **77:** 1091–1101.

Wever EG. 1972. Cochlear structure in the dolphin, *Lagenorhynchus obliquidens*. *Proceedings of the National Academy of Sciences of the United States of America* **69:** 657–661.

Wever EG, McCormick JG, Palin J, Ridgway SH. 1971. Cochlea of the dolphin, *Tursiops truncatus*: the basilar membrane. *Proceedings of the National Academy of Sciences of the United States of America* **68:** 2708–2711.

Yamato M, Ketten DR, Arruda J, Cramer S. 2008. Biomechanical and structural modeling of hearing in baleen whales. *Bioacoustics* **17:** 100–102.

SUPPORTING INFORMATION

Additional Supporting Information may be found online in the supporting information tab for this article:

Figure S1. Correlations (Spearman's Rho) of extant specimens and body mass and length.
Figure S2. Anterior views of the bony labyrinths of extant and extinct specimens examined. All specimens are from the left side of the body. Scale bar applies to all specimens.
Figure S3. Dorsal views of the bony labyrinths of extant and extinct specimens examined. All specimens are from the left side of the body. Scale bar applies to all specimens.
Table S1. Museum numbers, locality and life history data (when available), and novel CT scanning parameters for specimens used in this study.
Table S2. Dimensions and shape ratios of the bony labyrinths of phocoenids and selected delphinids used in this study. [Corrections added on 23rd August, 2016, after first online publication: Values in columns CT, Ap, and Cs of Table S2 have been amended, and consequently all affected measurements in the main text have been updated].
Table S3. Dimensions of the internal structures of the cochlear canal at each quarter of every turn.
Table S4. Dimensions and orientations of anterior (A), lateral (L), and posterior (P) semicircular canals.
Table S5. Dimensions and shape ratios of the bony labyrinths of phocoenids and selected delphinids used for low frequency hearing calculations.